Next Gen Multidisciplinary Research
ISSN (Online): 3108-1290
Volume 1, Issue 2 (July-December), 2025, 1-6

Research Article *Open Access*

Thickness-Driven Device Characteristics of $MAPbI_3$ Perovskite Solar Cells: Insights from SCAPS-1D Modelling

Ramakrishna Mahanta and Ipsita Mohanty*

Department of Physics, Dharanidhar University, Keonjhar, Odisha, India, 758001.

*Corresponding author email ID: ipsitamohanty8895@gmail.com

ARTICLE INFO

Article History:
Received: 3 September 2025
Accepted: 27 November 2025

Keywords:
Perovskite solar cells
SCAPS-1D simulation
Layer thickness optimization
$MAPbI_3$

ABSTRACT

The work assesses the effect of variable thickness on the output of planar $MAPbI_3$ perovskite solar cells (PSCs), studied using SCAPS-1D simulation. A planar heterojunction structure constituting Au/SnS/$MAPbI_3$/TiO_2/ZnO:Al has been proposed, and the thicknesses of the hole transport layer (HTL), absorber layer, and electron transport layer (ETL) were changed systematically to optimize the efficiency of the device. The thicknesses of HTL (SnS), perovskite absorber, and ETL (TiO_2) were adjusted between 0.1 and 1 µm. The simulations were carried out at standard AM1.5G sunlight, and several photovoltaic parameters, such as open-circuit voltage (V_{oc}), short-circuit current density (J_{sc}), Fill Factor (FF), and Power Conversion Efficiency (PCE), were studied. The optimization of the thickness of HTL (=0.3 µm), perovskite layer (=0.4 µm) and ETL (=0.2 µm) resulted in V_{oc} of 1.036 V, J_{sc} of 32.01 mA/cm², FF of 70.89% and overall efficiency of 23.50%. These findings illustrate that the layer engineering has a considerable impact on charge transportation, recombination behaviour, and overall device performance. The study highlights the potential of simulation-driven structural optimization to enhance the efficiency of planar $MAPbI_3$ PSCs.

1. INTRODUCTION

1.1. *Context and Significance of PSCs*

Energy demand is continuously increasing due to population expansion and rapid industrialization. This requirement has created pressure on conventional energy sources, leading to environmental pollution and the depletion of fossil fuels (Raimi et al., 2022). Consequently, renewable energy resources have evolved as a viable alternative to these traditional energy sources. Within the array of renewable energy sources, solar energy has gained significant importance because of its abundance, clean nature, and sustainability (International Energy Agency, 2025). Conventional silicon solar cells are costly and involve complex manufacturing processes, which limit their widespread use. To overcome these limitations, new solar cell technologies have been developed with improved efficiency and reduced cost.

In recent years, PSCs have garnered widespread interest in the field of photovoltaics due to their outstanding optoelectronic characteristics, low-cost fabrication techniques, and rapid increase (Chen et al., 2018; Oku, 2020). PSCs have shown a remarkable elevation in PCE from 3.8 % in 2009 to

https://doi.org/10.66132/mr010201

more than 27 % in a short period, which establishes their potential as next-generation solar cells (Im et al., 2011; Zhao et al., 2014; National Renewable Energy Laboratory [NREL], n.d.). Higher absorption coefficient, adjustable bandgap, larger carrier diffusion length, and low exciton binding energy establish PSCs as strong contenders for highly efficient and economically viable photovoltaic devices (Qaid et al., 2016; Khan & Panjwa, 2021).

1.2. *Context and Significance of Perovskite Solar Cells*

PSCs are generally classified into two types based on their device structure: mesoscopic and planar. In mesoscopic structures, a mesoporous layer (usually TiO_2) is used for electron transport, whereas planar structures do not have any mesoporous layer (Chen et al., 2018). The planar structure has advantages such as simple fabrication, reduced hysteresis, and suitability for flexible devices. In the present study, a planar heterojunction perovskite solar cell structure consisting of Au/SnS/$MAPbI_3$/TiO_2/ZnO:Al has been considered.

The device consists of five layers: a back contact (Au), a HTL of SnS, a $MAPbI_3$ layer, an ETL of TiO_2, and a front transparent conductive oxide (ZnO:Al). Each layer is an integral part of the operation of the solar cell. The perovskite layer absorbs photons and generates electron–hole pairs. The generated electrons are transported through the ETL towards the front electrode, while holes are transported through the HTL towards the back electrode. Efficient charge transport and collection depend on the energy level alignment and thickness of each layer (Oku, 2020; Zhao et al., 2014).

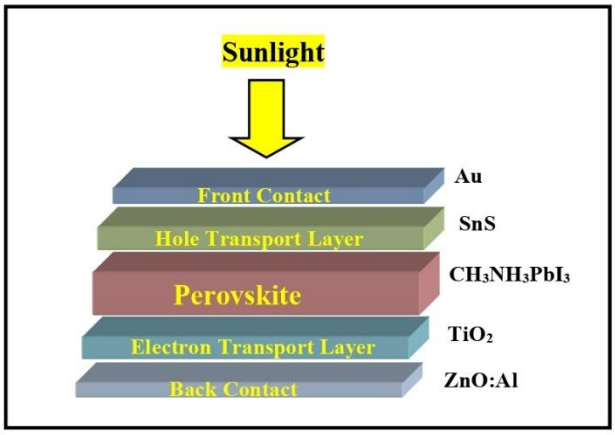

Figure 1. Device Architecture of the proposed PSC

Table 1. Physical Parameters used in Simulation (Mohanty et al., 2022)

Parameters	SnS	$CH_3NH_3PbI_3$	TiO_2	ZnO: Al
Thickness (μm)	0.3	0.4	0.2	0.1
Band gap, E_g (eV)	1.20	1.5	3.26	3.3
Electron Affinity (eV)	4.20	4.2	4.20	4.6
Relative Permittivity, ε_r	12.50	6.5	10.00	9.0
CB density of states (1/cm^3)	4.13×10^{19}	2.5×10^{20}	2.2×10^{18}	2.2×10^{18}
VB density of states (1/cm^3)	1×10^{19}	2.5×10^{20}	1.8×10^{19}	1.8×10^{19}
Electron Thermal Velocity (cm/s)	1×10^{7}	1×10^{7}	1×10^{7}	1×10^{7}
Hole Thermal Velocity (cm/s)	1×10^{7}	1×10^{7}	1×10^{7}	1×10^{7}
Electron Mobility, μ_e (cm^2/Vs)	1×10^{2}	5×10^{1}	1×10^{2}	1×10^{2}
Hole Mobility, μ_h (cm^2/Vs)	4	5×10^{1}	2.5×10^{1}	2.5×10^{1}
Donor Concentration, N_D(1/cm^3)	0	0	1×10^{19}	1×10^{18}
Acceptor Concentration, N_A (1/cm^3)	1.5×10^{20}	1×10^{13}	0	0

2. METHODOLOGY

For the present work, SCAPS-1D (Solar Cell Capacitance Simulator) software was employed for the simulation of PSCs. It is an initiative from the Department of Electronics and Information Systems, University of Gent, Belgium, designed for simulating $CuInSe_2$ and the CdTe family. However, its applicability has been expanded to include crystalline cells such as Si and GaAs, a-Si, and PSCs.

The following qualities of this software make it suitable for simulation purposes (Niemegeers et al., 2014):

- Seven semiconductor layers can be added.
- Three types of recombination mechanisms can be simulated.
- Various types of defect levels can be optimized.

- Contacts and work function can be varied.
- Intra-band and to and from interface state tunnelling can be applied.
- Multiple standard and additional illumination spectra are considered.
- Batch calculations are possible.
- Built-in curve-fitting functionality is available.

SCAPS-1D software is rooted in the solution of Poisson's equation, continuity equations and drift–diffusion equations.

The Poisson equation is given by:

$$\nabla \cdot (\varepsilon \nabla \phi) = -q(p - n + N_D^+ - N_A^-)$$

Where, ε is the permittivity of the material, ϕ is the electrostatic potential, q is the elementary charge, p is the hole concentration, n is the electron concentration, N_D^+ is the density of ionized donor atoms, and N_A^- is the density of ionized acceptor atoms.

The continuity equations are represented as:

$$\frac{\partial n}{\partial t} = \frac{1}{q}\nabla \cdot J_n + G - R$$

$$\frac{\partial p}{\partial t} = -\frac{1}{q}\nabla \cdot J_p + G - R$$

where $\frac{\partial n}{\partial t}$ = time derivative of the electron concentration, J_n = electron current density, G = rate of electron-hole pair generation, R = recombination rate, q = elementary charge, $\frac{\partial p}{\partial t}$ = time derivative of the hole concentration, and J_p = hole current density.

The current density equations are given by:

$$J_n = q\mu_n n\nabla\phi + qD_n\nabla n$$

$$J_p = q\mu_p p\nabla\phi - qD_p\nabla p$$

where J_n = electron current density, q = elementary charge, μ_n = electron mobility, n = electron concentration, ∇ϕ = gradient of electrostatic potential (electric field), D_n = electron diffusion coefficient, and ∇n = electron concentration gradient; similarly, J_p = hole current density, μ_p = hole mobility, p = hole concentration, D_p = hole diffusion coefficient, and ∇p = hole concentration gradient.

3. RESULTS AND DISCUSSION

3.1. Role of Layer Thickness

The thickness of different layers is essential in determining the overall performance of perovskite solar cells. The thickness of the absorber layer affects the amount of light absorbed, carrier generation, and recombination rates. An optimum thickness is required to ensure sufficient optimized light absorption and reduced charge-carrier recombination losses (Qaid et al., 2016). Similarly, the thickness of the HTL and ETL affects charge transport and collection.

If the HTL is too thin, it may not provide sufficient coverage, leading to increased recombination. On the other hand, if it is too thick, series resistance increases, which reduces the fill factor and overall efficiency. The ETL thickness also influences electron extraction and transport. A very thin ETL may cause incomplete coverage and poor electron transport, whereas a very thick ETL can increase resistance and reduce efficiency (Oku, 2020; Zhao et al., 2014). Therefore, the optimization of layer thickness is essential to achieve high PCE in planar PSCs. In this study, the SCAPS-1D simulation tool has been employed to systematically analyze the effect of varying the thicknesses of the HTL, absorber, and ETL layers on the photovoltaic performance of the Au/SnS/$MAPbI_3$/TiO_2/ZnO:Al device structure. The aim has been to determine the PCE that yields maximum efficiency under standard AM1.5G solar illumination conditions.

3.2. Optimisation of thickness of SnS

In the Au/SnS/$CH_3NH_3PbI_3$/TiO_2/ZnO:Al device, at first, the thickness of HTL was ranged from 0.1 µm to 1 µm to determine the optimal thickness for maximizing efficiency. During the initial optimization, the perovskite layer thickness was kept constant at 0.4 µm, the TiO_2layer was maintained at 0.2 µm, while the ZnO:Al layer was fixed at 0.1 µm. Figure 2 depicts the variation of thickness of SnS with the JV parameters. From the figure, it can be observed that V_{OC} Increases, J_{SC} increases, FF decrease sand the η increases with increase in thickness of SnS. The corresponding JV curve for thickness variation is shown in figure:3. After optimization, the thickness of SnS has been chosen to be 0.3 µm.

3.3. Optimisation of thickness of $CH_3NH_3PbI_3$

The thickness of the absorber layer significantly influences the overall functionality of a solar cell. To analyze its effect, the thicknesses of both absorber layers were systematically varied in the

device simulation. Specifically, the perovskite layer thickness was adjusted from 0.1 µm to 1 µm, and the corresponding simulation results are illustrated in Figure 4. As shown in the graphs, increasing the layer thickness alters the output characteristics. A thicker absorber layer enhances electron–hole pair generation resulting from improved absorption of longer wavelengths of light. When the absorber layer is thinner, electrons are more likely to recombine at the back contact, as the depletion region and back contact are in closer proximity.

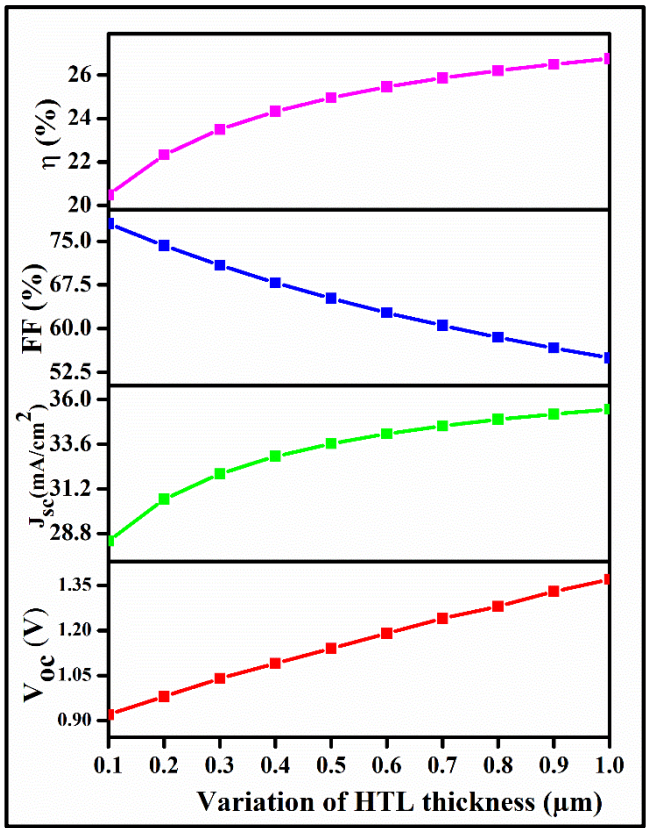

Figure 2. Variation of HTL thickness with JV parameters

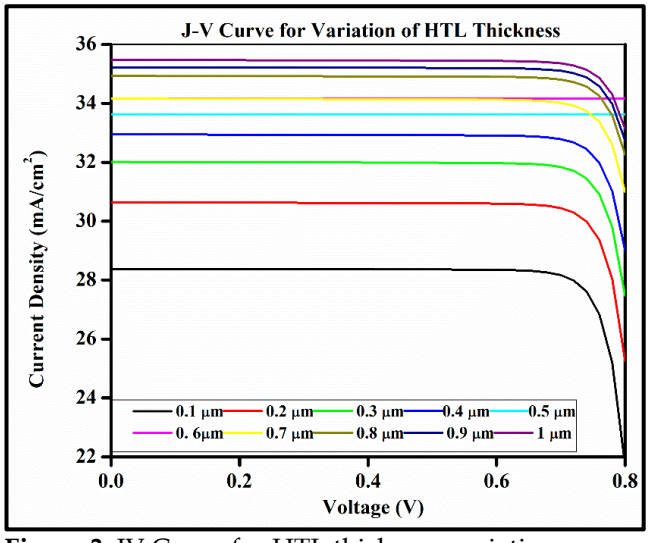

Figure 3. JV Curve for HTL thickness variation

With increasing absorber thickness, more photons are absorbed, resulting in higher electron–hole pair generation and enhanced electron mobility. Consequently, the V_{OC}, J_{SC}, and overall efficiency of the device increase. However, the FF is influenced by the electric field within the absorber, which weakens under higher forward bias, leading to reduced carrier collection and a lower FF as thickness increases. Therefore, optimizing the absorber thickness is essential to maximize output parameters while minimizing the reverse saturation current (Mohanty et al., 2021). Based on this optimization, the thickness of $CH_3NH_3PbI_3$ was selected to be 0.4 µm. The JV characteristics corresponding to variations in perovskite thickness are presented in Figure 5.

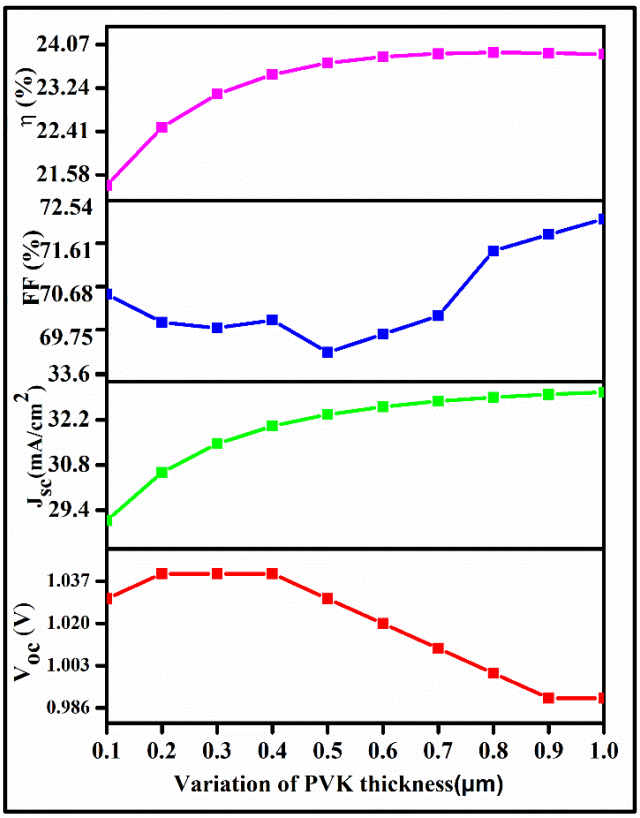

Figure 4. Variation of Perovskite thickness with JV parameters

3.4. Optimisation of thickness of TiO_2

In the Au/SnS/$CH_3NH_3PbI_3$/TiO_2/ZnO:Al device, at last, the thickness of ETL and was ranged from 0.1 µm to 1 µm to determine the optimal thickness for maximizing efficiency. During the initial optimization, the perovskite layer thickness was retained constant at 0.4 µm, the TiO_2 layer was maintained at 0.2 µm, while the ZnO:Al layer was fixed at 0.1 µm. Figure: 6 depicts the variation of thickness of TiO_2 with the JV parameters. From the figure, it can be observed that V_{OC} decreases, J_{SC} decreases, FF increases and the η exhibiting a

decreasing trend with increase in thickness of TiO_2. The corresponding JV curve for thickness variation is displayed in figure: 7. After optimisation, the thickness of TiO_2 has been chosen to be 0.2 µm.

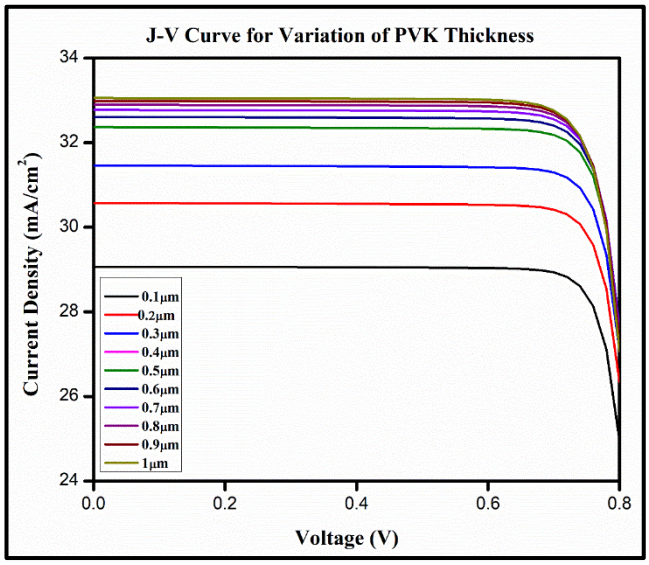

Figure 5. JV Curve for PVK thickness variation

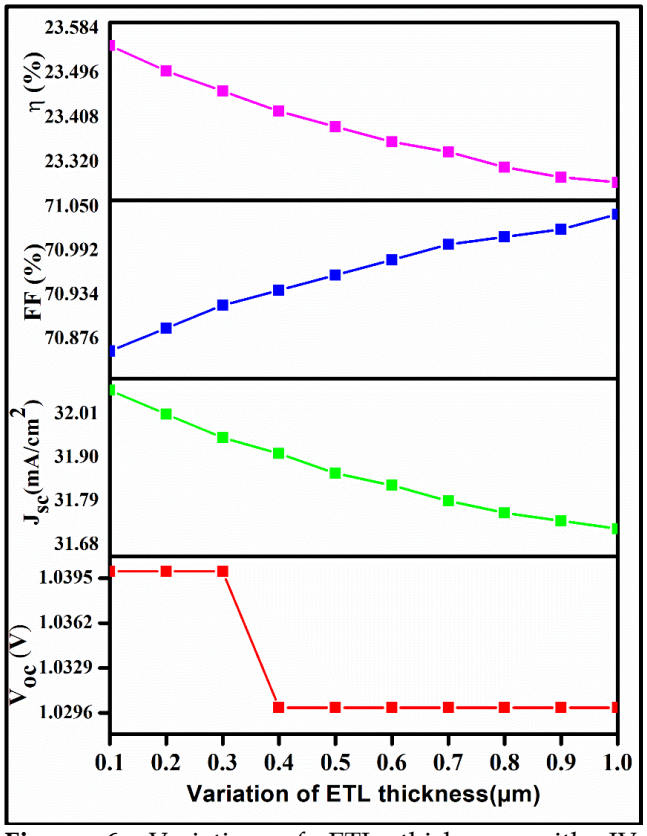

Figure 6. Variation of ETL thickness with JV parameters

3.5. Simulated Output

For the device structure, Au/SnS/$CH_3NH_3PbI_3$/ TiO_2/ZnO:Al, after optimising the thickness of HTL (SnS), Perovskite ($CH_3NH_3PbI_3$) and ETL (TiO_2) an output of V_{OC} = 1.036 V, J_{SC} = 32.01 mA/cm², FF = 70.89 % and η = 23.50 %. The final optimised result is plotted in figure 8.

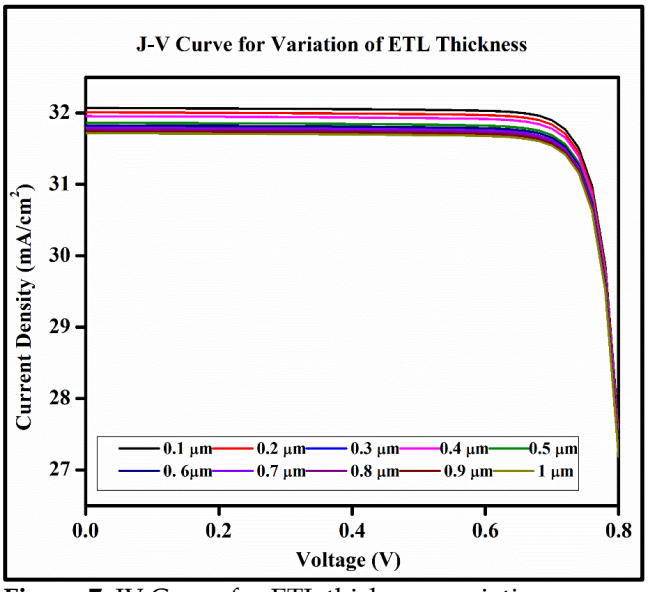

Figure 7. JV Curve for ETL thickness variation

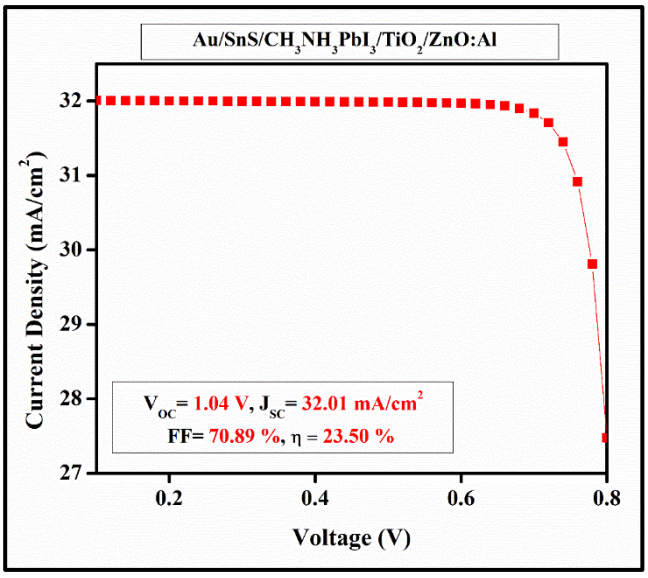

Figure 8. Final Optimised JV Curve

4. CONCLUSION

The numerical modelling of the PSC structure has been carried out using SCAPS-1D software to examine the influence of thickness on device performance. The effect of the absorber layer, HTL and ETL thickness has been evaluated. It has been observed that the J_{SC} increases with absorber thickness, while the V_{OC} shows a slight variation. The overall study has demonstrated that the optimisation of absorber, HTL and ETL thickness are essential for achieving higher efficiency and stability in PSCs.

Conflicts of Interest: The author declares no conflicts of interest.

Funding: This research received no external funding.

Acknowledgement: The authors express their gratitude to the staff of the Department of Physics, Dharanidhar University, Keonjhar, Odisha, for their support and cooperation during the study.

REFERENCES

Belarbi, M., Benyoucef, A., & Benyoucef, B. (2014). Simulation of the solar cells with PC1D: Application to cells based on silicon. *Advanced Energy: An International Journal (AEIJ), 1*(3), 1–11. https://doi.org/10.5121/aeij.2014.1301

Chen, Y., Zhou, N., & Zhou, H. (2018). Organic inorganic hybrid perovskite materials and devices. In Encyclopedia of Modern Optics II (Vol. 5). Elsevier. https://doi.org/10.1016/B978-0-12-409547-2.13499-8

Gong, J. (2021). Simulation of steady-state characteristics of heterojunction perovskite solar cells in wxAMPS. *Optik - International Journal for Light and Electron Optics, 232*, 166382. https://doi.org/10.1016/j.ijleo.2021.166382

Hima, A., Khechekhouche, A., Kemerchou, I., Lakhdar, N., Benhaoua, B., Rogti, F., Telli, I., & Saadoun, A. (2018). GPVDM simulation of layer thickness effect on power conversion efficiency of $CH_3NH_3PbI_3$ based planar heterojunction solar cell. *International Journal of Energetica (IJECA), 3*(1), 37–41. https://doi.org/10.46223/ijeeca.v3i1.191

Im, J.-H., Lee, C.-R., Lee, J.-W., Park, S.-W., & Park, N.-G. (2011). 6.5% efficient perovskite quantum-dot-sensitized solar cell. Nanoscale, 3(10), 4088. https://doi.org/10.1039/c1nr10867k

International Energy Agency. (2025). IEA Global Energy Review 2025 Report. Taiyang News. https://www.iea.org/reports/global-energy-review-2025

Khan, D., & Panjwa, M. K. (2021). A short report on up to date stability progress of perovskite solar cells. *Academia Letters*, Article 2261. https://doi.org/10.20935/AL2261

Mohanty, I., Mangal, S., & Singh, U. P. (2021). Performance optimization of lead free-MASnI3/CIGS heterojunction solar cell with 28.7% efficiency: A numerical approach. *Optical Materials, 122*, 111812. https://doi.org/10.1016/j.optmat.2021.111812

Mohanty, I., Mangal, S., & Singh, U. P. (2022). A numerical study on defect densities of double absorber CH3NH3PbI3/CIGS solar cell. *Materials Today: Proceedings, 62*, 987-991. https://doi.org/10.1016/j.matpr.2022.04.248

National Renewable Energy Laboratory (NREL). (n.d.). Best research-cell efficiency chart. https://www.nrel.gov/pv/cell-efficiency.html

Niemegeers, A., Burgelman, M., & Decock, K. (2014). SCAPS manual. University of Gent. https://scaps.elis.ugent.be/

Oku, T. (2020). Crystal structures of perovskite halide compounds used for solar cells. *Reviews on Advanced Materials Science, 59*, 264–305. https://doi.org/10.1515/rams-2020-0021

Press Information Bureau. (2025). Solar energy contributed the most... now stands at 105.65 GW. Government of India. https://pib.gov.in/PressReleasePage.aspx?PRID=2120729

Qaid, S. M. H., Al Sobaie, M. S., Khan, M. A. M., Bedja, I. M., Alharbi, F. H., Nazeeruddin, M. K., & Aldwayyan, A. S. (2016). Band-gap tuning of lead halide perovskite using a single step spin-coating deposition process. *Materials Letters, 164*, 498–501. https://doi.org/10.1016/j.matlet.2015.10.109

Raimi, D., Campbell, E., Newell, R., Prest, B., Villanueva, S., & Wingenroth, J. (2022). Global energy outlook 2022: Turning points and tension in the energy transition. *Resources for the Future.* https://www.rff.org/publications/reports/global-energy-outlook-2022

Stangl, R., Froitzheim, A., Kriegel, M., Elstner, L., & Fuhs, W. (2003). AFORS-HET: A computer program for the simulation of heterojunction solar cells to be distributed for public use. In *Proceedings of the 3rd World Conference on Photovoltaic Energy Conversion* (pp. 279–282). Osaka, Japan.

Zhao, Y., Nardes, A. M., & Zhu, K. (2014). Solid-state mesostructured perovskite $CH_3NH_3PbI_3$ solar cells: Charge transport, recombination, and diffusion length. *The Journal of Physical Chemistry Letters, 5*(3), 490–494. https://doi.org/10.1021/jz4021416